European Journal of Taxonomy 921: 210–235
https://doi.org/10.5852/ejt.2024.921.2429
ISSN 2118-9773
www.europeanjournaloftaxonomy.eu
2024 · Bellvert A. *et al.*

Research article

urn:lsid:zoobank.org:pub:02633F29-4CDF-4027-BEBF-07AD2F925B42

Integrating museum collections and molecules reveals genus-level synonymy and new species in red devil spiders (Araneae, Dysderidae) from the Middle East and Central Asia

Adrià BELLVERT [1,*], Dragomir DIMITROV [2], Alireza ZAMANI [3] & Miquel A. ARNEDO [4]

[1,2,4] Departament de Biologia Evolutiva, Ecologia i Ciències Ambientals, Universitat de Barcelona (UB), Av. Diagonal, 643, 08028 Barcelona, Spain.
[1,2,4] Institut de Recerca de la Biodiversitat (IRBio), Universitat de Barcelona (UB) Barcelona, Spain.
[2] National Museum of Natural Sciences, Bulgarian Academy of Sciences, 1 Tsar Osvoboditel Blvd, 1000 Sofia, Bulgaria.
[3] Zoological Museum, Biodiversity Unit, FI-20014 University of Turku, Finland.

[*] Corresponding author abellvertba@gmail.com
[2] Email: dimitrov.drk@gmail.com
[3] Email: zamani.alireza5@gmail.com
[4] Email: marnedo@gmail.com

[1] urn:lsid:zoobank.org:author:0ABC3DFE-E982-47F5-A5DA-732688BCDEA9
[2] urn:lsid:zoobank.org:author:37EC22F1-6348-4A61-B55F-3E74498AE5E9
[3] urn:lsid:zoobank.org:author:A21C0B82-E2D9-4402-9408-D6160843DAF4
[4] urn:lsid:zoobank.org:author:0148CECC-0BCF-469F-8614-F4A447C26408

Abstract. This paper reviews little-known species of the dysderid spider genera *Dysdera* Latreille, 1804, and *Dysderella* Dunin, 1992 based on specimens collected in the Caucasus, Middle East, and Central Asia. After combining molecular phylogeny of five mitochondrial and three nuclear genes with morphological evidence, *Dysderella* is proposed as a junior synonym of *Dysdera*. In addition, three species are described as new to science: *D. jaegeri* Bellvert & Dimitrov sp. nov., *D. naouelae* Bellvert & Dimitrov sp. nov., and *D. kourosh* Bellvert, Zamani & Dimitrov sp. nov. Four combinations are proposed: *Dysdera caspica* Dunin, 1990 comb. rev., *Dysdera transcaspica* Dunin & Fet, 1985 comb. rev., *Dysdera elburzica* (Zamani, Marusik & Szűts, 2023) comb. nov. and *Dysdera sancticedri* (Brignoli, 1978) comb. nov. (ex. *Dasumia* Thorell, 1875). Furthermore, we report a first record of *D. festai* Caporiacco, 1929 in Turkey and its male cheliceral polymorphism. Our results illustrate the deficiencies that undermine the current taxonomy of this genus. For example, many species are described based on only one or few specimens or limited locality data. The advancements in DNA sequencing technologies applied to museum specimens reduce the need for fieldwork collection and export of fresh specimens. This highlights the significance of museum collections for improving research in this field.

Keywords. Taxonomy, molecular phylogeny, polymorphism, integrated taxonomy, taxonomic impediment.

Bellvert A., Dimitrov D., Zamani A. & Arnedo M.A. 2024. Integrating museum collections and molecules reveals genus-level synonymy and new species in red devil spiders (Araneae, Dysderidae) from the Middle East and Central Asia. *European Journal of Taxonomy* 921: 210–235. https://doi.org/10.5852/ejt.2024.921.2429

Introduction

Dysderidae C.L. Koch, 1837 is a large family of spiders, currently comprising 612 extant species in 25 genera, distributed in the West Palearctic (World Spider Catalog 2023). The taxonomy of Dysderidae remains problematic. Almost one-third of the genera are monotypic, many of which have not been even reported again since their original description, in some cases more than 100 years ago, and in at least one case the type specimen is immature (World Spider Catalog 2023). One-third of the species are known by only one sex. Some descriptions lack a proper diagnosis (see *Dysderella* Dunin, 1992 below) or are poorly illustrated – e.g., most of Eugène Simon's papers, who described over 100 dysderid species. The female vulva, which is the main source of specific diagnostic traits for females was not regularly documented until the 1960s by the pioneering works of Alicata (1964), over 150 years after the description of the first dysderid. With very few exceptions (e.g., Alicata 1964; Deeleman-Reinhold & Deeleman 1988), there has been no revisionary work conducted, and most studies describe either single or few species or are focused on restricted geographic areas (e.g., Řezáč *et al.* 2023). Similarly, molecular phylogenetic hypotheses are only available for some of the genera (e.g., Bidegaray-Batista & Arnedo 2011) and particular regions (e.g., Arnedo *et al.* 2001).

Most of these limitations are particularly acute for the species distributed in the easternmost regions of its range, such as Anatolia, the Levant, Caucasus, the Middle East and Central Asia. The genus *Dysderella* exemplifies this situation well. When describing the genus, Dunin (1992) did not provide any diagnosis. The original description only pointed out some similarities with *Dysdera* Latreille, 1804, but no specific differences were mentioned. Similarly, the two main eastern species groups of *Dysdera* – *asiatica* and *aculeata* – have never been properly diagnosed, as some authors already noted (Deeleman-Reinhold & Deeleman 1988; Dimitrov 2021). Many species have published non-valid diagnostic characters, poor illustrations, outdated descriptions, or their type specimens are lost. Accessing some type specimens kept in different collections in Russia and Turkey ranges from very difficult to impossible. Resolving taxonomic problems, due to unavailability of type material or missing information on one sex, requires the study of additional specimens. Similarly, expanding distribution ranges or gathering DNA sequence data for classification and testing evolutionary hypotheses relies on the availability of more specimens. Unfortunately, obtaining collection and exportation permits from certain countries can create obstacles for fieldwork.

Given the aforementioned limitations, museum collections remain the primary available source of material from these regions. It is essential to recognize that the use of museum specimens has certain weaknesses. The specimens currently held in museums were typically gathered several decades ago, rendering them unsuitable for sequencing using Sanger methodologies. However, advancements in sequencing technologies may greatly assist in resolving this issue (Raxworthy & Smith 2021). Moreover, they frequently lack important information about the specific locality, habitats, or even the collection date and collector. Despite these shortcomings, the study of museum collections can expose mistakes as well as inaccurate taxonomic (e.g., Scharff & Hormiga 2013; Holmgren *et al.* 2016; Ernst *et al.* 2022) and phylogenetic decisions (e.g., Twort *et al.* 2021), substantially enhancing our current knowledge of biodiversity.

In this study, we primarily examined museum specimens to revise several species of the dysderid subfamily Dysderinae from the Middle East and Central Asia. Based on morphological and molecular evidence, we synonymize a genus, describe three new species, propose four new combinations, and discover a new faunistic record (Fig. 1).

Material and methods

The studied material was primarily sourced from various museum collections and preserved in 70–75% ethanol. Specimens were examined using a LEICA MZ16A stereoscopic microscope equipped with a camera lucida. High-resolution digital images were captured using a LEICA DFC 450 digital camera and the Leica Application Suite ver. 4.4 software program, and a FLIR digital camera equipped with a THORLABS C-mount CML15 lens and attached to a ZEISS Axio LAB.A1 microscope. Helicon Focus software program was used to stack the photographs. LAS ver. 4.4 was used to take measurements from the scaled images, and both male palps and female vulvae were dissected to allow for further examination. The genitalia were enzymatically digested in a pancreatin and borax solution following the methodology of Alvarez-Padilla & Hormiga (2007) to remove membranous tissues and retain sclerotized parts. The description of the new species was recorded in DELTA format, as specified by Dallwitz (1980) and Dallwitz *et al.* (2020). The nomenclature of genitalic and copulatory structures follows Arnedo *et al.* (2000). Leg chaetotaxy was recorded according to the techniques utilized in previous studies that focused on the revision and description of species of *Dysdera* from the Canary Islands (Arnedo & Ribera 1996, 1997, 1999; Arnedo *et al.* 2007; Macías-Hernández *et al.* 2010). All measurements are in mm and coordinates in decimal format.

Abbreviations

Morphology

Somatic characters:

AME = anterior median eye
B = basal tooth
d = dorsal
D = distal tooth
fe = femur
M = medial tooth
me = metatarsus
pa = patella
PLE = posterior lateral eyes
PME = posterior median eyes
ta = tarsus
ti = tibia
v = ventral

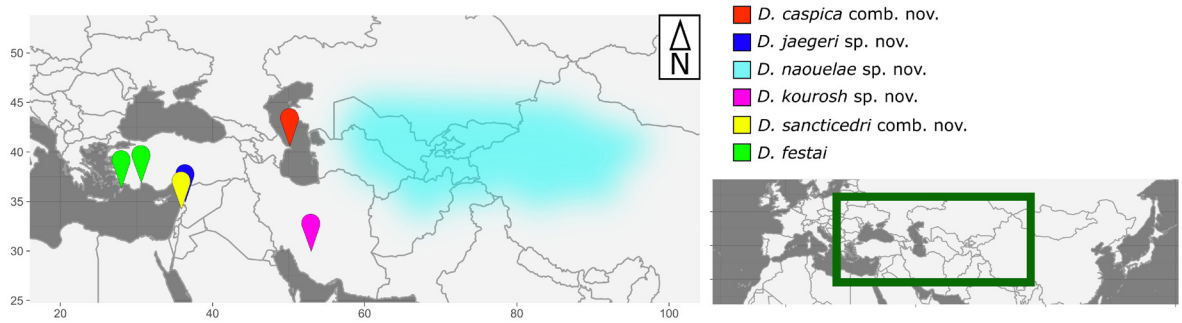

Fig. 1. Map of the geographical distribution of the studied specimens. Blurred area represents the species with unknown exact locations.

Male copulatory organ:
AC = additional crest
AL = additional lateral sheet
AS = anterior sclerite
C = crest
DH = distal haematodocha
ED = embolic division
ES = external sclerite
F = flagellum
IS = internal sclerite
L = lateral sheet
LA = lateral sheet apophysis
LF = lateral fold
LML = lateral margin of the lateral sheet
P = posterior apophysis
Pdp = pedipalp
T = tegulum

Female genitalia:
AVD = additional ventral diverticulum
DA = dorsal arch
DF = dorsal fold
MF = major fold
S = spermatheca
TB = transversal bar
VA = ventral arch

Institutions (curators noted in brackets)
CRBA = Centre de Recursos de Biodiversitat Animal, University of Barcelona, Spain (T. Serra)
MCSN = Museo Civico di Storia Naturale, Verona, Italy (L. Latella)
MZSUT = Museo Regionale di Scienze Naturali, Torino, Italy (L. Giraldi)
NHMW = Naturhistorisches Museum, Vienna, Austria (C. Hörweg)
SMF = Naturmuseum Senckenberg, Frankfurt am Main, Germany (P. Jäger)

Molecular procedures and phylogenetic analysis

DNA extraction, amplification, and sequencing were performed following Crespo *et al.* (2020). Five mitochondrial genes, namely cytochrome c oxidase subunit I (COI), 12S rRNA, 16S rRNA, tRNA Leu (L1), NADH dehydrogenase subunit 1 (NAD1), and three nuclear genes, namely 28S rRNA, 18S rRNA, and histone 3 (H3), were targeted. The newly generated sequences were combined with the sequences of Dysderidae available in GenBank. These sequences were automatically retrieved using the R package phylotaR (Bennett *et al.* 2018). Additional outgroup species within the superfamily Dysderoidea and closely related families, Caponiidae Simon, 1890 and Trogloraptoridae Griswold, Audisio & Ledford, 2012, were also included.

The sequences were edited, and the matrices were manipulated using Geneious Prime ver. 2022.2.2 (www.geneious.com). Ribosomal genes were aligned using the automatic alignment algorithm G-INS-i as implemented in the online version of MAFFT ver. 7 (Katoh & Standley 2013). COI, NAD1, and H3 were aligned using the translation align option with the cost matrix BLOSUM62. The single gene matrices were then concatenated into a single supermatrix using the program SequenceMatrix ver. 1.7.8 (Vaidya *et al.* 2011). The supermatrix was analyzed under maximum likelihood, Bayesian inference,

and parsimony. Maximum likelihood tree was inferred using the program IQTREE ver. 2.1.2 (Minh *et al.* 2020), which selected the best partition scheme and evolutionary models with MODELFINDER (Kalyaanamoorthy *et al.* 2017) and assessed nodal support with 1000 iterations of ultrafast bootstrap (Hoang *et al.* 2018). Bayesian inference was conducted with MrBayes ver. 3.2.6 (Ronquist *et al.* 2012), and the best partition scheme and evolutionary models were estimated using the program Partition Finder ver. 2.1.1 (Lanfear *et al.* 2017). The analysis was run for 10 million generations, sampling every 1000, with eight simultaneous Markov Chain Monte Carlo (MCMC) chains, a heating temperature of 0.15, and a relative initial burn-in of 25%. Support values were calculated as posterior probabilities. Convergence of the chains, correct mixing, and the number of burn-in generations were monitored using Tracer ver. 1.7 (Rambaut *et al.* 2018). Parsimony analysis of the concatenated matrix was conducted with the program TNT ver. 1.5 (Goloboff & Catalano 2016). For parsimony analyses, gaps were recoded as absence / presence characters using the simple coding method proposed by Simmons & Ocheterena (2000) implemented in the computer program SeqState (Müller 2005). Following Soto *et al.* (2017), we use a combination of the 'New Technologies' search strategies in TNT, namely sectorial searches, tree fusing, drift and ratchet. Tree searches were driven to hit independently 10 times the optimal scoring, followed by tree bisection and reconnection (TBR) branch swapping. Support values were estimated by jack-knifing frequencies derived from 1000 resampled matrices using 15 random addition sequences, retaining 20 trees per replication, followed by TBR, and TBR collapsing to calculate the consensus. All trees were rooted assuming Caponiidae as the sister group to the remaining families (Michalik *et al.* 2019). The phylogenetic trees were edited using FIGTREE (http://tree.bio.ed.ac.uk/software/figtree/).

Results

Molecular phylogeny

One specimen each of *Dysderella caspica* (Dunin, 1990) and *Dysdera kourosh* sp. nov. yielded DNA extractions of enough quality for subsequent target amplification. In addition, a specimen of *Dysdera longirostris* Doblika, 1853 was also sequenced for the target gene fragments to test the morphological affinities of *D. caspica* with the *longirostris* species group. A list of sequences generated and retrieved from GenBank along with accession numbers for the newly generated sequences are available in Supp. file 1. The final supermatrix included 166 taxa and 5711 characters. Results of the phylogenetic analyses under alternative inference methods are summarized in Fig. 2. The best trees with supports for maximum likelihood, Bayesian inference and parsimony are available in Supp. file 2. Preferred partition schemes and corresponding evolutionary models are available in Supp. file 3. All analyses agreed on including *D. caspica* within the genus *Dysdera*, as the sister of *D. longirostris* and related to other representatives of the *longirostris* species group. Surprisingly, *D. kourosh* was not recovered as closely related to other eastern species. Instead, all analyses agreed, with low support in parsimony, to place it within a clade exclusively including representatives from the westernmost part of the genus distribution range. One possible explanation could be that no other representative of the *aculeata* group was available for comparison. This illustrates well the importance of performing an integrative study of the genus east of the Balkans.

Taxonomy

Class Arachnida Cuvier, 1812
Order Araneae Clerck, 1757
Family Dysderidae C.L. Koch, 1837

Genus ***Dysdera*** Latreille, 1804

Dysderella Dunin, 1992: 67 (type species: *Dysdera transcaspica* Dunin & Fet, 1985), **syn. nov.**

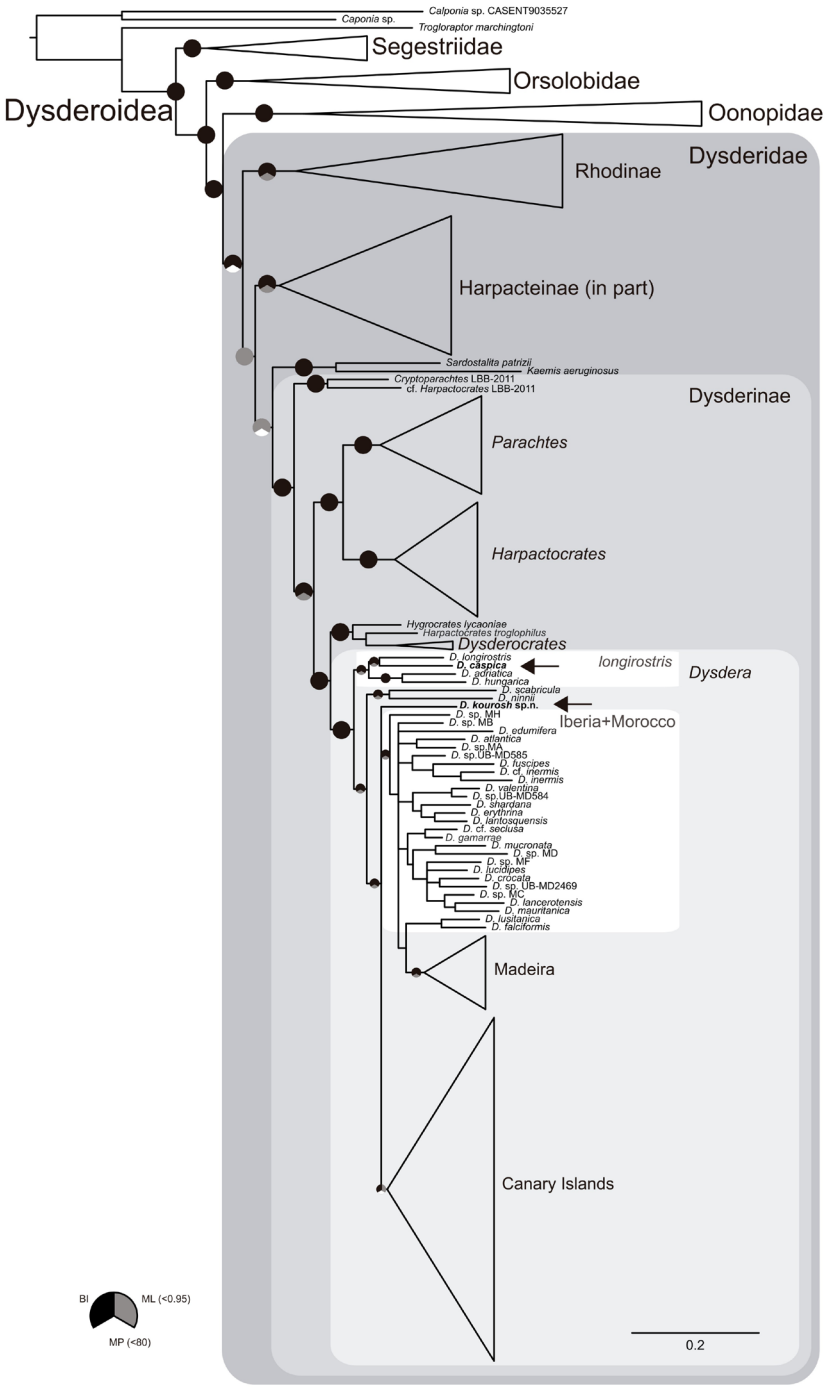

Fig. 2. Preferred maximum likelihood tree of Dysderoidea C.L. Koch, 1837. Species and clades are boxed according to taxonomic groupings or geographic regions. Node support results from analyses under alternative inference methods are summarized using pie charts on branches. Upperleft pie = Bayesian inference (BI; MrBayes), Upperright pie = Maximum Likelihood (ML; IQTree2), Lower pie = Parsimony (MP; TNT). Support levels are color coded as follows: black = node recovered with high support (PP > 0.95, ML ultrafast bootstrap support > 95, Parsimony jackknife > 80); gray = node recovered but support values below thresholds indicated before; white = node not recovered. GenBank accession numbers in Supp. file 1.

Remarks

Dunin (1992) described the genus *Dysderella* and transferred the species *Dysdera caspica* and *Dysdera transcaspica* Dunin & Fet, 1985 to it. He designated *D. transcaspica* as the type species of this genus. However, he did not explicitly transfer it as a new combination, nor did he provide diagnostic differences to distinguish *Dysderella* from *Dysdera*. Zamani *et al.* (2023a) diagnosed and redescribed the genus *Dysderella* and described one more species, namely *D. elburzica.* The diagnosis of the genus they proposed, in our opinion, is not correct. According to the authors, it differs from *Dysdera* by the smaller size (i.e., carapace < 2.1 mm vs > 4 mm) and the spineless legs I and II. We think, the size is not a reliable diagnostic character for Dysderidae. There are some small-sized species of *Dysdera*, like *D. zonsteini* Dimitrov, 2021 with size of the carapace 1.65 mm. The spineless legs I and II are typical for the *Dysdera longirostris* species group (Deeleman-Reinhold & Deeleman 1988) and this character does not separate the two genera either. The molecular analysis shows that *D. caspica* belongs to the *longirostris* group of *Dysdera* (sensu Deeleman-Reinhold & Deeleman 1988). We could not sequence D. *transcaspica* and *D. elburzica*, but due to their high morphological resemblance to *D. caspica*, they should also fall in this group. Additionally, the three species share morphological features with *Dysdera*, such as scopulae on the posterior metatarsi, claw tufts on all tarsi, and a notched anterior edge of the labium. They also share the spineless legs I and II with *D. longirostris* species group which further supports the results from the molecular analyses. Thus, we propose to transfer the three of them back to *Dysdera* and consider *Dysderella* as a junior synonym of *Dysdera*.

Dysdera caspica Dunin, 1990 comb. rev.
Figs 3–5

Dysdera caspica Dunin, 1990: 143, fig. 4.1–4.

Dysderella caspica – Dunin 1992: 67, fig. 12 (transfer from *Dysdera*).

Diagnosis

See Dunin (1990: 143).

Material examined

AZERBAIJAN • 1 ♂; Baku Region Absheron Peninsula, near Baku; 40.490556° N, 50.151667° E; 18 Jun. 2003; Y.M. Marusik leg.; CRBA crba000530.

Description

Male (Figs 3–5**)**

Prosoma. 1.88 long; maximum width 1.47; minimum width 0.95. Uniformly red; slightly wrinkled, anterior region smooth. Frontal border roughly round, ca ½ of carapace length; anterior lateral borders convergent; rounded at maximum dorsal width, posterior lateral borders rounded; posterior margin narrow, rounded. Eye diameters: AME 0.12; PLE 0.11; PME 0.10; AMEs on edge of frontal border, separated from one another by ca 1 diameter, touching PLEs; PMEs ca one-quarter of diameter apart, less than ¼ of PME diameter from PLEs. Labium trapezoid-shaped, its base wider than its distal part, borders slightly curved; longer than wide at base; semi-circular notch at tip. Sternum orange, frontally darker, becoming lighter posteriorly; smooth; uniformly covered with slender black setae.

Chelicerae. 0.84 long, ca ½ of carapace length in dorsal view; fang 0.80 long; paturon proximal dorsal and ventral side scantly covered with piligerous granulations. Cheliceral inner groove short, ca ⅓ of cheliceral length; armed with three teeth and lamina at base; B = M > D; D triangular, located roughly at centre of groove; B close to basal lamina; M close to B.

Legs. Orange. Lengths of leg segments (leg 2 missing): fe1 1.45; pa1 0.91; ti1 1.11; me1 1.14; ta1 0.42; total 5.05; fe3 0.98; pa3 0.58; ti3 0.60; me3 0.85; ta3 0.29; total 3.30; fe4 1.33; pa4 0.78; ti4 1.01; me4 1.21; ta4 0.38; total 4.73; fe Pdp 0.88; pa Pdp 0.54; ti Pdp 0.42; ta Pdp 0.53; total 2.37; leg formula: 1>4>3. Fe3d spineless; pa3 spineless; tb3d spines arranged in one band; proximal 0; medial-proximal 0; medial-distal 0; distal 1.0.0; tb3v spineless; with one terminal spine on forward margin. Fe4d spineless; pa4 spineless; tb4d spineless; tb4v spineless; with one terminal spine at anterior border. Dorsal side of frontal legs covered with small thin grains; ventral side of pedipalp covered with setae, lacking grains. Claws with 8 teeth or less.

Opisthosoma. Cream-coloured. Abdominal dorsal hairs 0.03 long; thin, slightly curved, not compressed, pointed; uniformly and thickly distributed.

Palp (Figs 3–5). T markedly shorter than ED; external distal border straight; internal sloped backward. ED slightly bent in lateral view; internal distal border not expanded. IS and ES equally developed, fused basally; IS and ES continuous to tip, bent ventrally. ED tip straight in lateral view. C present, long; distal border rounded, smooth, slightly expanded, projected over ED external part. AC absent. LF absent. L poorly developed; external border sclerotized, not folded. LA absent. F present, distally curved. AL present, very poorly developed; proximal border in posterior view fused with DH. Base of P fused to T; slightly sloped upwards; lateral length from ⅓ to ⅔ of T width; ridge present, perpendicular to T; not expanded, upper margin smooth; not distally projected; posterior margin not folded.

Female

Not examined. See Dunin, 1990.

Figs 3–5. Male *Dysdera caspica* Dunin, 1990 comb. rev. (crba000530 CRBA), left palp (F broken on 3 and 4). **3**. Prolateral view. **4**. Anterior view. **5**. Retrolateral view. Scale bar = 0.5 mm.

Distribution

Azerbaijan.

Dysdera transcaspica Dunin & Fet, 1985 comb. rev.

For diagnosis and description see Dunin (1990) and Zamani *et al.* (2023a).

Dysdera elburzica (Zamani, Marusik & Szűts, 2023) comb. nov.

For diagnosis and description see Zamani *et al.* (2023a).

Dysdera jaegeri Bellvert & Dimitrov sp. nov.
urn:lsid:zoobank.org:act:579D5ABE-98BC-4B60-96DC-721AA2C027FE
Figs 6–8

Diagnosis

Male resembles that of *Dysdera sultani* Deeleman-Reinhold & Deeleman, 1988 by having the external and internal sclerites fused in a single anterior sclerite, surrounding the lateral sheet (Fig. 7), and the bent embolic division (Figs 7–8). The two species can be distinguished by (1) the short and stout lateral sheet with transparent lamellar extension in *D. jaegeri* sp. nov. (Fig. 8), vs thin and long single processus in *D. sultani* (Deeleman-Reinhold & Deeleman 1988: figs 236–237), (2) less bent embolic division (i.e., ca 60°) in *D. jaegeri*, vs ca 80° in *D. sultani*, (3) the apical part of the embolic division is a whole plate in *D. jaegeri* (Figs 6, 8), while in *D. sultani* it is sulcate apically, and (4) the posterior apophysis in *D. jaegeri* is more or less straight, perpendicular to the tegulum (Figs 6, 8), vs long and more bent towards the tegulum in *D. sultani* (Deeleman-Reinhold & Deeleman 1988: fig. 236).

Etymology

This species is named after our colleague and reputed German arachnologist Peter Jäger.

Type material

Holotype

SYRIA • 1 ♂; Homs Province, west of Homs, ruins and abandoned cemetery NW of the castle; 18 Mar. 1973; R. Kinzelbach leg.; SMF.

Description

Male (Figs 6–8)

Prosoma. 3.13 long; maximum width 2.32; minimum width 1.61. Reddish, uniformly; with small dark grains mainly in frontal part; frontally covered with small white setae. Frontal border roughly round, ca ½ of carapace length; anterior lateral borders parallel; rounded at maximum dorsal width, back lateral borders rounded; back margin narrow, bilobulated. Eye diameters: AME 0.17; PLE 0.15; PME 0.14; AMEs on edge of frontal border, separated from one another by ca ½ diameter, close to PLEs; PMEs very close to one another, ca ⅓ of PME diameter from PLEs. Labium trapezoid-shaped, base wider than distal part; as long as wide at base; semicircular groove at tip. Sternum orange-red, frontally darker, becoming lighter posteriorly; smooth; uniformly covered with slender black setae.

Chelicerae. 1.13 long, ca ⅓ of carapace length in dorsal view; fang medium-sized, 0.88 long; paturon dorsal and ventral side completely covered with piligerous granulations. Cheliceral inner groove short,

ca ⅓ of cheliceral length; armed with three teeth and lamina at base; B > M > D; D triangular, located roughly at centre of groove; B close to basal lamina; M close to B.

Legs. Anterior legs orange, posterior legs yellow. Lengths of leg segments: fe1 2.36; pa1 1.49; ti1 1.87; me1 2.06; ta1 0.58; total 8.36; fe2 2.14; pa2 1.38; ti2 1.68; me2 1.95; ta2 0.56; total 7.72; fe3 1.65; pa3 0.94; ti3 1.00; me3 1.45; ta3 0.51; total 5.59; fe4 2.04; pa4 1.48; ti4 1.46; me4 1.97; ta4 0.62; total 7.58; fe Pdp 1.50; pa Pdp 0.88; ti Pdp 0.57; ta Pdp 0.91; total 3.86; leg formula: 1 > 2 > 4 > 3. Leg2 spineless. Fe3d spineless; pa3 spineless; tb3d spines arranged in two bands; proximal 1.0.0-1; medial-proximal 0; medial-distal 0; distal 1.0.1; tb3v spines arranged in two bands; proximal 1-2.0.0; medial-proximal 0; medial-distal 0; distal 1-0.0.0; with one terminal spine on forward margin. Fe4d spines in two rows; forward 1; backward 2; pa4 spineless; tb4d spines arranged in two bands; proximal 1.0.1; medial-proximal 0; medial-distal 0; distal 0.0.1; tb4v spines arranged in two bands; proximal 1.1.0; medial-proximal 0; medial-distal 0; distal 0-1.0.0; with one terminal spine at the distal border. Dorsal side of frontal legs smooth; ventral side of pedipalp smooth. Claws with 8 teeth or less; hardly larger than claw width.

Opisthosoma. 3.87 long; cream-colored; cylindrical. Abdominal dorsal setae 0.04 long; thin, almost straight, pointed; uniformly and thickly distributed.

Palp (Figs 6–8). T slightly longer than ED; external distal border straight, internal projected at middle. ED bent ca 60 degrees in lateral view, internal distal border markedly expanded. IS and ES completely fused, forming a single anterior sclerite (Fig. 7). ED tip straight in lateral view. C present, short and

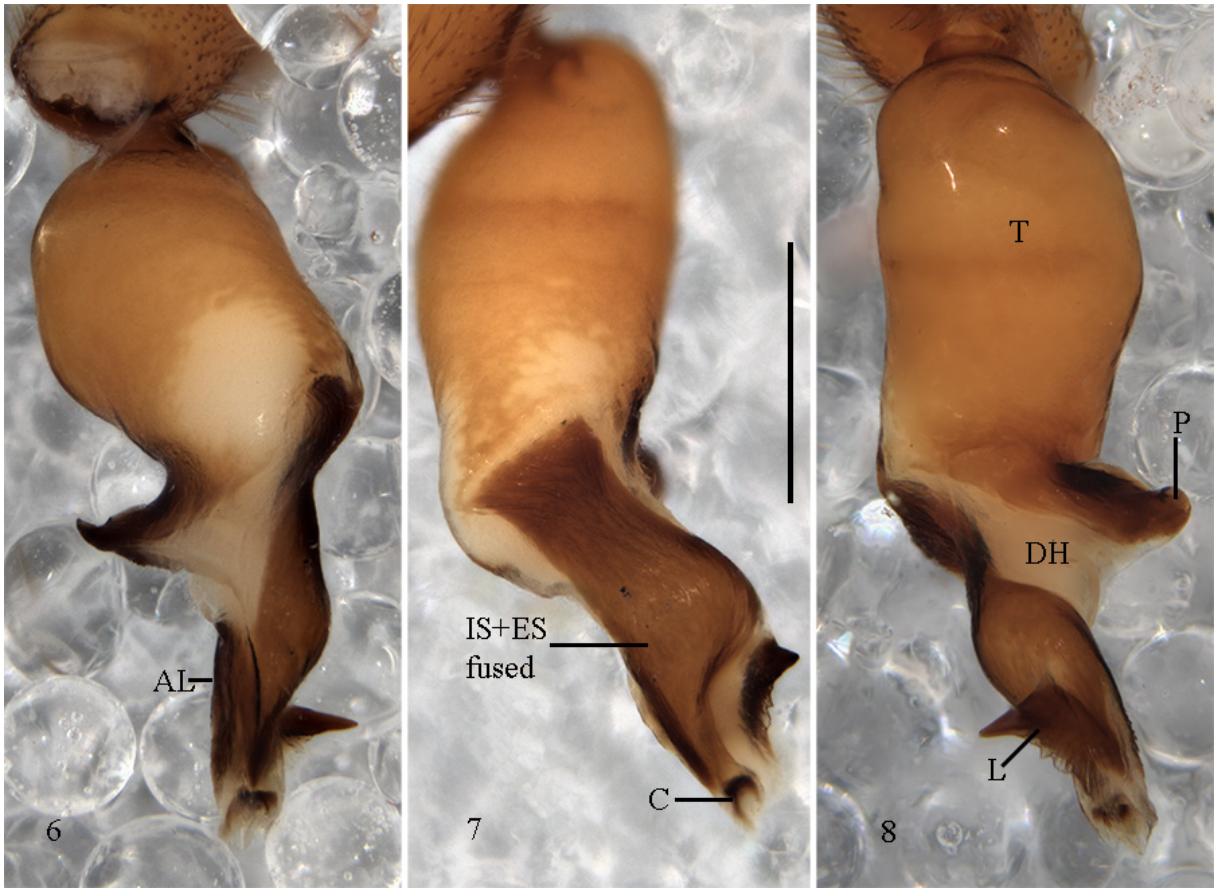

Figs 6–8. Male *Dysdera jaegeri* Bellvert & Dimitrov sp. nov. (SMF), left palp. **6**. Prolateral view. **7**. Anterior view. **8**. Retrolateral view. Scale bar = 0.5 mm.

poorly developed, located in distal end on ED internal tip, proximal border of C continuously decreasing. LF absent. L well developed, anteriorly not projected with a spine-like basal projection. External border poorly sclerotized, forming a transparent ridge between spine-like apophysis and distal part, not folded. AL present, well developed; proximal border in posterior view smooth, not fused with distal haematodocha. P short, fused to T; lateral length of P from ⅖ to ½ of T width; ridge present, perpendicular to T; distinctly expanded, rounded, upper margin smooth; distally ridge-like expanded; posterior margin not folded.

Female

Unknown.

Distribution

Known only from the type locality in Homs Province, central Syria.

Remarks

Dysdera jaegeri sp. nov. along with *D. argaeica* Nosek, 1905, *D. sultani*, *D. galinae* Dimitrov, 2018 and *D. yozgat* Deeleman-Reinhold, 1988 form a complex of species within the diverse *asiatica* group that can be characterized by the long cylindrical T, entirely fused IS and ES, and the sclerotized processus-like lateral sheet. This complex is distributed in Turkey and Syria. Unfortunately, we were unable to sequence any of these species and their position in the Dysderinae tree remains unclear.

Dysdera naouelae Bellvert & Dimitrov sp. nov.
urn:lsid:zoobank.org:act:65B05A67-B976-49F1-A9E3-110A537035BE
Figs 9–14

Dysdera tartarica – Lazarov 2009: 104, figs 1–5 [misidentification].

Diagnosis

The new species is morphologically most similar to *Dysdera kourosh* sp. nov., *Dysdera mikhailovi* Fomichev & Marusik, 2021, and *Dysdera sagartia* Zamani, Marusik & Szűts, 2023 by the well-developed, wide and rounded crest (Figs 9–11), internal sclerite significantly wider than the exterior one, and the characteristic lateral margin of the lateral sheet (Fig. 10). The male differs by (1) the thin, well sclerotized processus-like lateral margin of the lateral sheet, almost perpendicular to the embolic division tip (Fig. 11), vs pointed backward in *D. kourosh* (arrowed in Fig. 20) and significantly wider in *D. mikhailovi* (Fomichev & Marusik 2021: fig. 46) and *D. sagartia* (Zamani *et al.* 2023b: fig. 19a), (2) the convex crest, with wider apical part (Fig. 9), vs concave at the middle in *D. kourosh* (Fig. 18) and wider in the basal part than in the apical part in *D. mikhailovi* (Fomichev & Marusik 2021: fig. 44), and (3) proximal border of the additional lateral sheet not fused with distal haematodocha (Figs 9, 11), vs fused in the other 2 species. Female differs by the curved spermatheca in dorsal view (Fig. 12), vs straight in *D. mikhailovi* (Fomichev & Marusik 2021: fig. 54) and the presence of a sclerotized neck in the spermatheca of *D. naouelae* sp. nov. (Fig. 14).

Etymology

The new species is named after Naouel El Jaarani Oualkadi, partner of the first author, for all her patience and support.

Type material

Holotype

"TURKESTAN" • 1 ♂; precise country, collection date and collector unknown; SMF.

Paratype

"TURKESTAN" • 1 ♀; precise country, collection date and collector unknown; SMF.

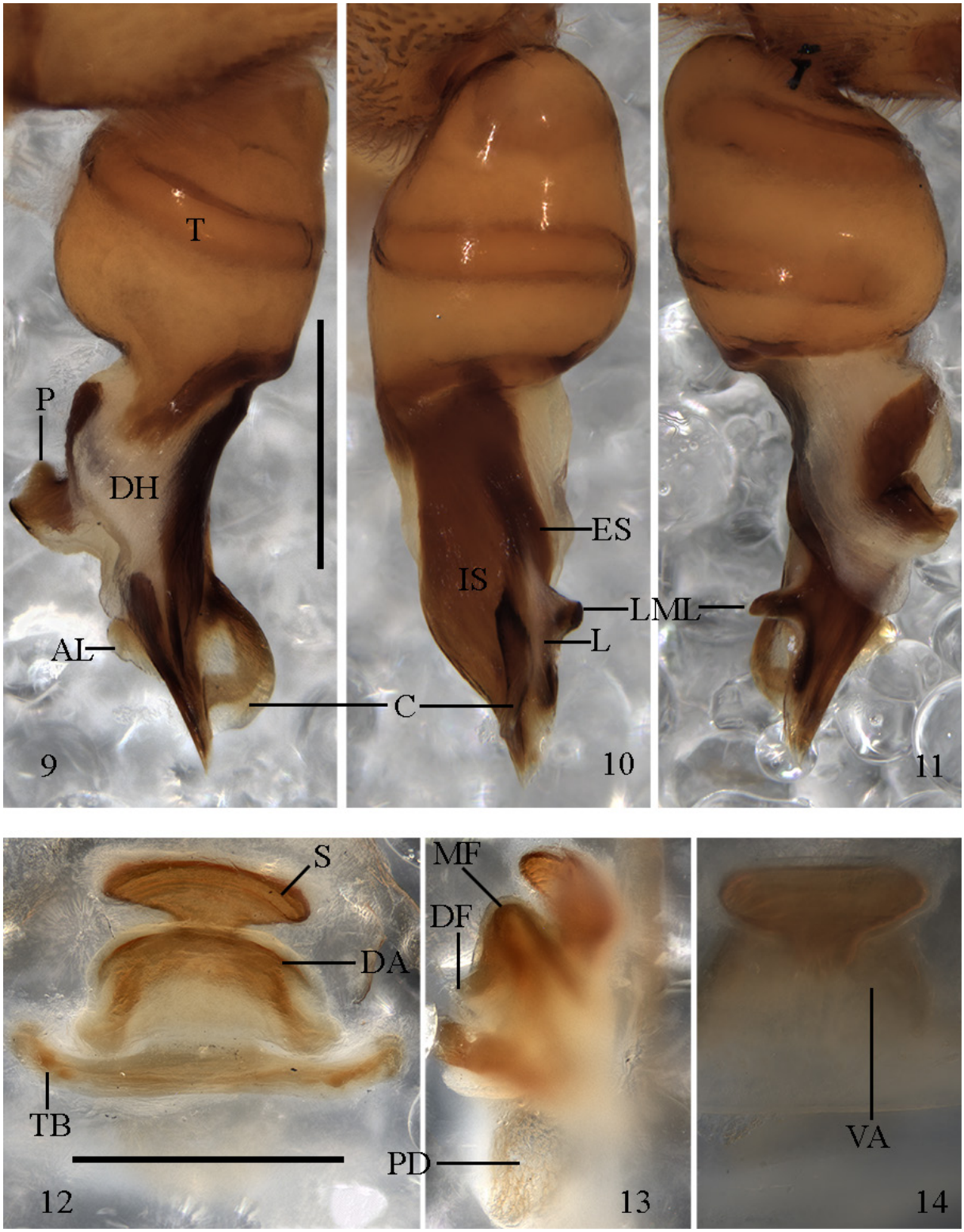

Figs 9–14. 9–11. Male *Dysdera naouelae* Bellvert & Dimitrov sp. nov. (SMF). **9**. Prolateral view. **10**. Anterior view. **11**. Retrolateral view. **12–14**. Female *Dysdera naouelae* Bellvert & Dimitrov sp. nov. (SMF), vulva. **12**. Ventral view. **13**. Lateral view. **14**. Dorsal view. Scale bars = 0.5 mm.

Comparative material examined

***Dysdera tartarica* Kroneberg, 1875** (Figs 15–17)

KYRGYZYSTAN • 1 ♂; Jalal-Abad Region, Ferganski range, Arslanbob; 12 Jun. 1983; S.L. Zonstein leg.; NHMW.

Description

Male (Figs 9–11)

Prosoma. 3.55 long; maximum width 2.63; minimum width 1.63. Uniformly orange-red; smooth with some small black grains mainly at front. Frontal border roughly triangular, about ½ of carapace length; anterior lateral borders convergent; rounded at maximum dorsal width, back lateral borders rounded; posterior margin narrow, straight. Eye diameters: AME 0.18; PLE 0.14; PME 0.11; AMEs on edge of the frontal border, separated from one another by about ⅔ diameter, close to PLEs; PMEs very close to one another, about ⅓ of PME diameter from PLEs. Labium trapezoid-shaped, base wider than the distal part; longer than wide at base; semi-circular groove at the tip. Sternum orange, frontally darker, becoming lighter towards the back; wrinkled; covered with setae mainly on margin.

Chelicerae. 1.36 long, about ⅔ of carapace length in dorsal view; fang medium-sized, 0.99 long; paturon dorsal and ventral side completely covered with piligerous granulations. Cheliceral inner groove short, about ⅓ of cheliceral length; armed with three teeth and lamina at base; B > D = M; D triangular, located roughly at the centre of the groove; B close to basal lamina; M close to B.

Legs. Front legs orange, back legs yellow. Lengths of leg segments: fe1 2.85; pa1 1.81; ti1 2.40; me1 2.65; ta1 0.67; total 10.38; fe2 2.62; pa2 1.65; ti2 2.17; me2 2.48; ta2 0.61; total 9.52; fe3 2.03; pa3 1.12; ti3 1.30; me3 1.98; ta3 0.52; total 6.94; fe4 2.74; pa4 1.40; ti4 1.93; me4 2.57; ta4 0.66; total 9.30; fe Pdp

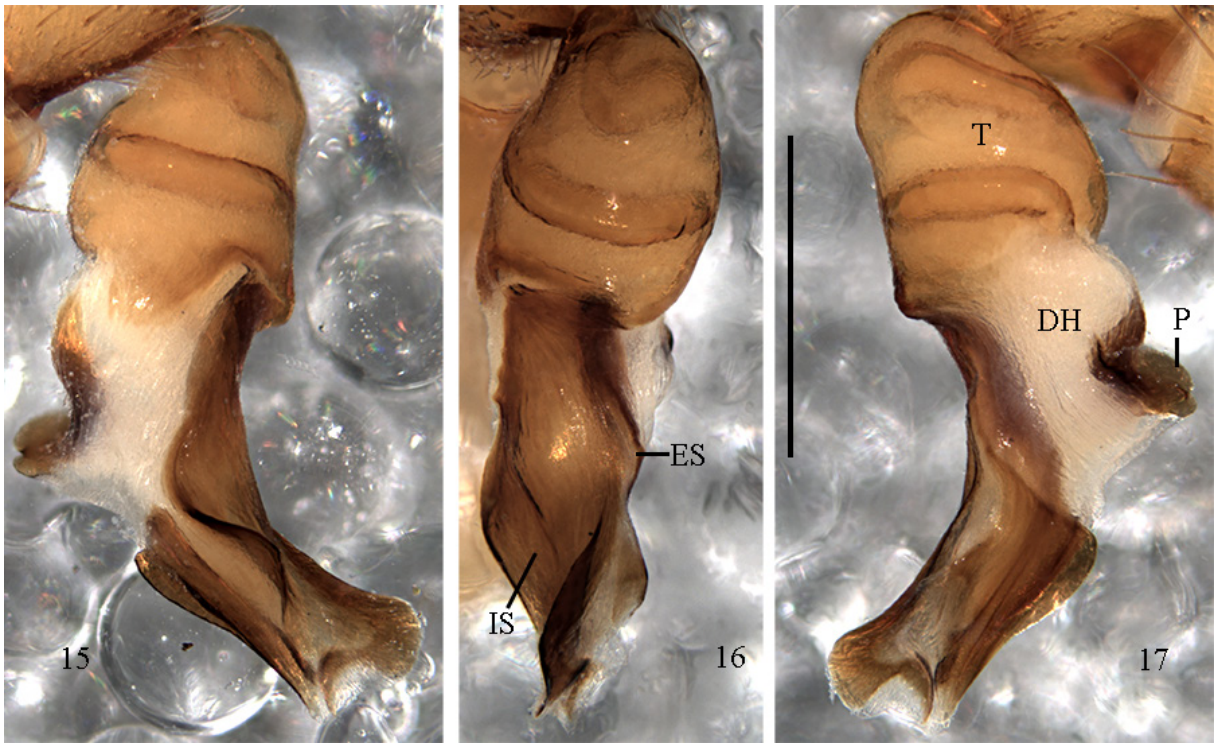

Figs 15–17. Male *Dysdera tartarica* Kroneberg, 1875 (NHMW), left palp. **15**. Prolateral view. **16**. Anterior view.**17**. Retrolateral view. Scale bar = 0.5 mm.

1.67; pa Pdp 0.94; ti Pdp 0.81; ta Pdp 0.93; total 4.35; leg formula: 1>2>4>3. Leg 1 has two terminal spines on the forward margin; leg 2 two terminal spines on the forward margin. Fe3d spines in two rows; forward 2; backward 1; pa3 spineless; tb3d spines arranged in two bands; proximal 1.0.1; medial-proximal 0; medial-distal 0; distal 1.0.1; tb3v spines arranged in four bands; proximal 0.1.0; medial-proximal 1.1.0; medial-distal 0.1.0; distal 1.0.0; with two terminal spines. Fe4d spines in two rows, forward 2; backward 6-5; pa4 spineless; tb4d spines arranged in two bands; proximal 1.0.1; medial-proximal 0; medial-distal 0; distal 1.0.1; tb4v spines arranged in four bands; proximal 1.2.0; medial-proximal 1.1.0; medial-distal 0.1.0; distal 1.0.0; with two terminal spines. Dorsal side of the frontal legs smooth; ventral side of the pedipalp covered with small piligerous grains. Claws with 8 teeth or less; hardly larger than claw width.

Opisthosoma. 3.76 long; cream-colored; cylindrical. Abdominal dorsal setae 0.02 long; thick, roughly straight, blunt, tip not enlarged; uniformly and thickly distributed.

Palp (Figs 9–11). T slightly shorter than ED, external distal border sloped forwards, internal one sloped backward. ED not bent, same T axis in lateral view, internal distal border not expanded. IS wider than ES, both more or less parallel; IS continuous to tip (Fig. 10). ED tip sloped towards back in lateral view. C present, long; distal end beside ED internal tip; distal border rounded, smooth, markedly expanded, perpendicular to ED (Fig. 9). AC absent. LF absent. L well developed, with a sclerotized processus-like basal lateral apophysis. LA absent. F absent. AL present, well developed; proximal border in posterior view smooth, not fused with distal haematodocha. P not fused to T (Fig. 9); lateral length from ⅔ to as long as T width; ridge present, parallel to T; not expanded, upper margin smooth; distally ridge-like expanded; posterior margin not folded.

Female (Figs 12–14)

Prosoma. 3.77 long; maximum width 2.73; minimum width 1.75. Orange, anteriorly darker, becoming lighter towards posterior. Anterior border almost round. Eye diameters: AME 0.19; PLE 0.11; PME 0.15, separated from one another by about 1 diameter and about ½ PME diameter from PLEs. Sternum uniformly orange.

Chelicerae. 1.53 long; 1.18. Cheliceral inner groove short, about ⅓ of cheliceral length; armed with three teeth and lamina at base; B>D>M.

Legs. Lengths of leg segments: fe1 2.74; pa1 1.81; ti1 2.17; me1 2.26; ta1 0.61; total 9.61; fe2 2.51; pa2 1.69; ti2 2.02; me2 2.19; ta2 0.55; total 8.96; fe3 1.96; pa3 1.13; ti3 1.32; me3 1.87; ta3 0.49; total 6.78; fe4 2.61; pa4 1.38; ti4 1.93; me4 2.53; ta4 0.56; total 9.01; fe Pdp 1.66; pa Pdp 0.80; ti Pdp 0.77; ta Pdp 0.94; total 4.18; leg formula 1>4>2>3. Leg 1 one terminal spine on forward margin. Fe3d spines in one row; 3; tb3v spines arranged in three bands; proximal 1.1.1; medial-proximal 1.1.1; medial-distal 0; distal 1.0.0; with two terminal spines. Fe4d spines in two rows; forward 3-2; backward 6-5; tb4v spines arranged in four bands; proximal 1.1.1-0; medial-proximal 1.1.0; medial-distal 0.0-1.0-1; distal 1.1-0.0; with two terminal spines.

Opisthosoma. 4.41 long. Abdominal dorsal hairs 0.08 long. All other somatic characters as in male.

Vulva (Figs 12–14). DA wider than long, fused to VA (Fig. 13); DF wide in dorsal view. MF margins fused, sheet-like, well developed, and completely sclerotized. VA rectangular, transparent (Fig. 14); frontal region completely sclerotized; posterior region sclerotized except for most internal area; AVD absent. S attachment projected under VA; arms as long as DA (Fig. 12), distinctly curved; tips not projected; neck as wide as arms. Laterals of TB directed forward.

Distribution

Central Asia (“Turkestan”).

Remarks

This species belongs to the *aculeata* group (sensu Deeleman-Reinhold & Deeleman 1988). It was erroneously recorded as *Dysdera tartarica* Kroneberg, 1875 by Lazarov (2009). We examined the male specimen of *D. tartarica*, described and depicted by Deeleman-Reinhold & Deeleman (1988), which fits the original description and the drawing of Charitonov (1956: 22, fig. 2). As clearly seen from its photographs (Figs 15–17), it is not conspecific with *D. naouelae* sp. nov. (Figs 9–14).

Dysdera kourosh Bellvert, Zamani & Dimitrov sp. nov.
urn:lsid:zoobank.org:act:2242E86D-6C29-47C0-883C-A7A549D8039E
Figs 18–20

Diagnosis

Dysdera kourosh sp. nov. resembles *D. naouelae* sp. nov., *D. mikhailovi*, and *D. sagartia* by the well-developed, wide crest, interior sclerite significantly wider than the exterior one, and the characteristic lateral margin of the lateral sheet. The male differs by (1) the lateral margin of the lateral sheet pointed dorsally (Fig 20), vs thin, sharp, more sclerotized and almost perpendicular to the embolic division in *D. naouelae* (Fig. 14), and significantly wider in *D. mikhailovi* (Fomichev & Marusik 2021: fig. 46), and *D. sagartia*, and (2) the concave crest (Fig. 18), vs rounded and not notched in the other three species.

Etymology

The specific epithet is a noun in apposition after Cyrus the Great – Kourosh in Persian, which translates as Lord of the Sun – the founder of the first Persian empire.

Type material

Holotype

IRAN • 1 ♂; Fars Province, Jahrom; 29.75° N, 52.68° E; 25 Mar. 2013; SMF.

Description

Male (Figs 18–20)

Prosoma. 2.77 long; maximum width 2.11; minimum width 1.37. Red, frontally darker, becoming lighter towards the back; smooth with some small black grains mainly at the front. Anterior border roughly round, about ½ of carapace length; anterior lateral borders convergent; rounded at maximum dorsal width, posterior lateral borders rounded; posterior margin narrow, straight. Eye diameters: AME 0.13; PLE 0.10; PME 0.10; AMEs on edge of the anterior border, separated from one another by about 1 diameter, close to PLEs; PMEs very close to one another, less than ¼ of PME diameter from PLEs. Labium trapezoid-shaped, its base wider than its distal part, borders slightly curved; longer than wide at base; semicircular groove at the tip. Sternum orange, darkened on borders; very slightly wrinkled, mainly between legs and anterior border; uniformly covered in slender black setae.

Chelicerae. 1.26 long, about ½ of carapace length in dorsal view; fang 1.12 long; paturon dorsal and ventral side completely covered with piligerous granulations. Cheliceral inner groove medium-size, about ⅔ of cheliceral length; armed with three teeth and lamina at base; D = B > M; D triangular, located near segment tip; B close to basal lamina; M close to B. Legs orange. Lengths of leg segments: fe1 2.36; pa1 1.45; ti1 2.00; me1 2.06; ta1 0.56; total 8.43; fe2 2.04; pa2 1.29; ti2 1.73; me2 1.92; ta2 0.49; total 7.48; fe3 1.59; pa3 0.89; ti3 1.08; me3 1.57; ta3 0.51; total 5.64; fe4 2.04; pa4 1.07; ti4 1.59; me4 1.98; total 6.69; fe Pdp 1.38; pa Pdp 0.73; ti Pdp 0.63; ta Pdp 0.70; total 3.45; leg formula: 1 > 2 > 4 > 3. Spination: palp: one spine on pa, three spines on fe distal internal; leg1 two terminal spines on forward margin; leg2 one terminal spine on the forward margin. Fe3d spines in two rows; forward 2; backward 1; pa3

1 ventral; tb3d spines arranged in two bands; proximal 1.0.1; medial-proximal 0; medial-distal 0; distal 1.0.1.; tb3v spines arranged in three bands; proximal 0.1.0; medial-proximal 1.1.0; medial-distal 0; distal 1.0.0; with two terminal spines. Fe4d spines in two rows; forward 1; backward 5; pa4 1 ventral medial; tb4d spines arranged in two bands; proximal 1.0.1; medial-proximal 0; medial-distal 0; distal 1.0.1; tb4v spines arranged in three bands; proximal 0.1.1; medial-proximal 1.1.0; medial-distal 0; distal 1.0.0; with two terminal spines. Dorsal side of the frontal legs covered with small piligerous grains; ventral side of the pedipalp covered with small piligerous grains. Claws with 8 teeth or less; hardly larger than claw width.

Opisthosoma. 2.54 long; cream-colored. Abdominal dorsal setae 0.02 long; thick, slightly curved, compressed, blunt, tip not enlarged; uniformly, thickly distributed.

Palp (Figs 18–20). T slightly shorter than ED; external distal border straight; internal sloped backward. ED the same T axis in lateral view, internal distal border not expanded. IS wider than ES, continuous to tip (Fig. 19). ED tip sloped towards back in lateral view. C present, long, slightly concave at the middle, seen from lateral view (Figs 18, 20); distal border round, the posterior border with a small sclerotized apophysis, markedly expanded, perpendicular to ED. AC absent. LF absent. L well developed; external border sclerotized, not folded, with processus-like basal lateral apophysis. LA absent. F absent. AL present, very poorly developed; proximal border in posterior view fused with DH. P not fused to T; perpendicular to T in lateral view; lateral length from ⅔ to ½ of T width; ridge present, parallel to T; not expanded, upper margin smooth, distally ridge-like expanded, back margin slightly folded towards the internal side.

Female

Unknown.

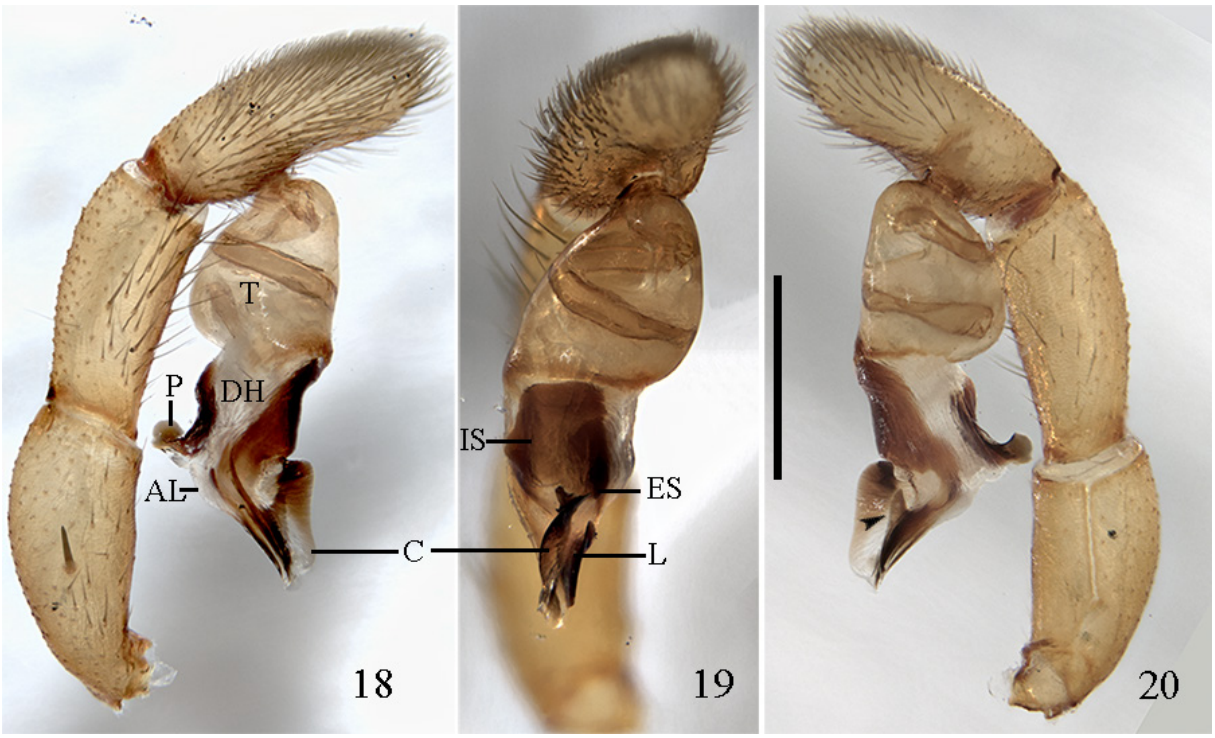

Figs 18–20. Male *Dysdera kourosh* Bellvert, Zamani & Dimitrov sp. nov. (SMF), left palp. **18**. Prolateral view. **19**. Anterior view. **20**. Retrolateral view. Scale bar = 0.5 mm.

Distribution

Known only from the type locality in Fars Province, southern Iran.

Remarks

The species belongs to the *aculeata* group (sensu Deeleman-Reinhold & Deeleman 1988).

Dysdera sancticedri (Brignoli, 1978) comb. nov.
Figs 21–25

Dasumia sancticedri Brignoli, 1978: 174, figs 1–2.

Diagnosis

Dysdera sancticedri comb. nov. resembles *Dysdera festai* (Caporiacco, 1929) by the conformation of the male palp, having a similar external sclerite. The two species differ by (1) the lack of a posterior apophysis in *D. sancticedri* (Figs 23, 25), vs present in *D. festai* (Fig. 28), (2) the reduced, hollow interior sclerite with a tubular shape in *D. sancticedri* (Fig. 24), vs well developed and connected basally to the exterior one in *D. festai* (Fig. 29), (3) the short, rounded tegulum, wider than long in *D. sancticedri* (Figs 23, 25), vs more elongated and longer than wide in *D. festai* (Figs 28–30), and (4) the long chelicerae, about ⅗ of carapace length in dorsal view in *D. sancticedri* (Figs 21–22), vs significantly smaller in *D. festai* (Figs 26–27).

Type material

Holotype

LEBANON • 1 ♂; North Gorvernorate, des Cèdres de Bacharré (caza Bcharré); 1950 m a.s.l.; 5 Jun. 1972; P. Brignoli leg.; MCSN.

Description

Male

Prosoma. 2.70 long; maximum width 2.14; minimum width 1.53. Uniformly red; cephalic region smooth, thorax heavily covered with circular depressions. Anterior border roughly round, about ⅗ of carapace length; anterior lateral borders divergent; rounded at maximum dorsal width, posterior lateral borders rounded; posterior margin narrow, slightly bilobulated. Eye diameters: AME 0.167; PLE 0.129; PME 0.122; AMEs on edge of the anterior border, separated from one another by about ¾ diameter, touching PLEs; PMEs very close to one another, about ⅓ of PME diameter from PLEs. Labium trapezoid-shaped, base wider than the distal part; as long as wide at base; triangular groove at the tip. Sternum dark orange, darkened on borders; very slightly wrinkled.

Chelicerae. 1.62 long, about ⅗ of carapace length in dorsal view; fang 1.865 long; paturon smooth, with no granulations (Figs 21–22). Cheliceral inner groove not visible; armed with slender long setae at the base.

Legs. Orange. Lengths of leg segments: fe1 2; pa1 1.29; ti1 1.73; me1 1.72; ta1 0.71; total 8.45; fe2 1.70; pa2 1.14; ti2 1.40; me2 1.44; ta2 0.63; total 6.31; fe3 1.37; pa3 0.85; ti3 0.91; me3 1.12; ta3 0.44; total 4.69; fe4 1.83; pa4 1.07; ti4 1.41; me4 1.58; ta4 0.49; total 6.38; fe Pdp 1.27; pa Pdp 0.76; ti Pdp 0.64; ta Pdp 0.81; total 3.48; leg formula: 1 > 4 > 2 > 3. Leg2 spineless; leg4 spineless. Fe3d spineless; pa3 spineless; tb3d spines arranged in one band; proximal 0; medial-proximal 0; medial-distal 0; distal 1.0.0; tb3v spines spineless; without terminal spines. Dorsal side of frontal legs covered with setae, lacking small grains; ventral side of pedipalp smooth. Claws with less than 5 teeth; hardly larger than claw width.

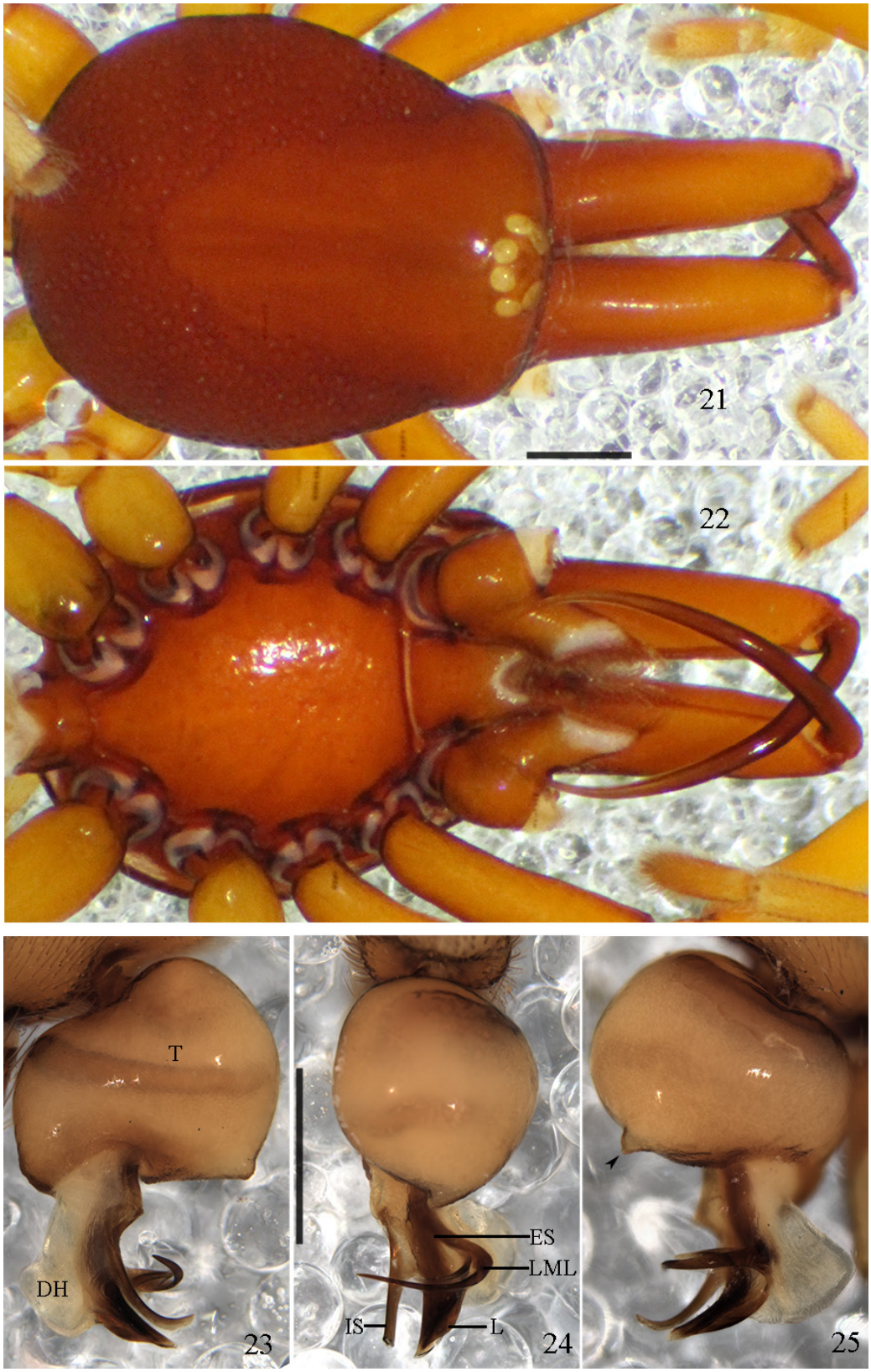

Figs 21–25. Male *Dysdera sancticedri* (Brignoli, 1978) comb. nov. (MCSN). **21–22**. Carapace. **21**. Dorsal view. **22**. Ventral view. **23–25**. Left palp. **23**. Prolateral view. **24**. Anterior view. **25**. Retrolateral view; arrowhead showing a small knob on the anterior side of T. Scale bars: 21–22 = 1.5 mm; 23–25 =0.5 mm.

Opisthosoma. 3.57 long; cream-colored; cylindrical. Abdominal dorsal setae 0.03 long; thin, roughly straight, not compressed, pointed; uniformly and thickly distributed.

Palp (Figs 23–25). T short and rounded, slightly longer than ED, bearing small knob on the anterior side (arrowed in Fig. 25); external distal border sloped forwards; internal sloped backward. ED not bent, same T axis in lateral view, internal distal border not expanded. ES wide markedly sclerotized, IS reduced to whip-like sclerotization (Fig. 24). ED tip reduced, only the sclerotized structures are visible. C absent. AC absent. L lateral margin distally projected, split into two spine-like apophyses (Fig. 24). L is a single well-developed apophysis, curved mesally. LA absent. F absent. AL absent. P absent (Figs 23, 25); DH sloped, forming an angle of ca 135° to T in lateral view; lateral length ca ¼ of T width; ridge ca 45° to T in lateral view, not sclerotized; not expanded, upper margin smooth; not distally projected; back margin not folded.

Distribution

Known only from the type locality in the North Governorate, northern Lebanon.

Remarks

The complete absence of a posterior apophysis is a unique feature of this species. Because of the overall resemblance of the male palp to that of *D. festai*, it most likely belongs to the *festai* group. However, it differs from the other two species in this group by the elongated chelicerae. To determine its correct position in the phylogeny of *Dysdera*, it is necessary to collect fresh material and describe the female too.

Dysdera festai Caporiacco, 1929
Figs 26–33

Diagnosis

See Deeleman-Reinhold & Deeleman (1988).

Type material

Neotype

GREECE • 1 ♂; South Aegean: Rhodes, Petaloudes; 15 Oct. 1984; P.R. Deeleman leg.; MZSUT.

Other material examined

GREECE • 1 ♂, 1 ♀, 5 juvs; South Aegean: Rhodes, Petaloudes; 15 Oct. 1984; P.R. Deeleman leg.; MZSUT.

TURKEY • 1 ♂; Antalya Province, Antalya; 13 May 1969; NHMW.

Description

See Deeleman-Reinhold & Deeleman (1988).

Distribution

Known from Greece (Rhodes), and the new record in Turkey reported herein.

Remarks

The chelicerae of the male collected from Turkey are unmodified (Fig. 26) while all the male specimens from the type locality bear a distinct projection at the middle part of the prolateral margin of the paturon (Fig. 27). There are two possible explanations for this phenomenon: either it is due to trait polymorphism,

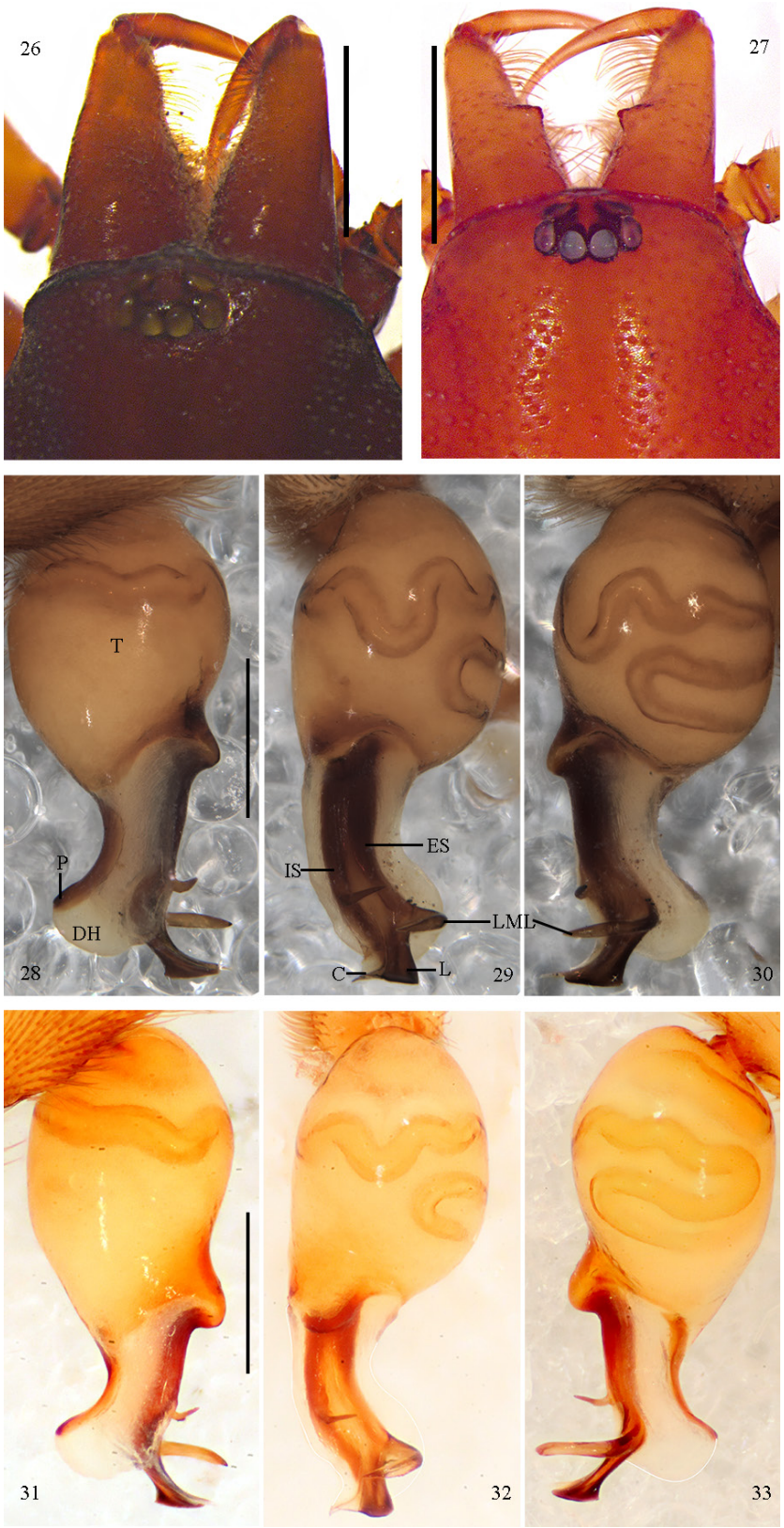

Figs 26–33. Male *Dysdera festai* Caporiacco, 1929 (26, 28–30 = specimen from Turkey (NHMW); 27, 31–33 = specimen from Greece (MZSUT)). **26–27**. Cephalic region. **28–33**. Left palp. **28, 31**. Prolateral view. **29, 32**. Anterior view. **30, 33**. Retrolateral view. Scale bars: 26–27 = 2 mm; 28–33 = 0.5 mm.

or the population from mainland Anatolia belongs to a different species altogether. The presence of a tooth-like prolateral projection on the male chelicera has been reported in other, unrelated species of *Dysdera* such as *Dysdera dentichelis* Simon, 1882 from Lebanon or *Dysdera mucronata* Simon, 1911 from Morocco, and in those species it is considered a diagnostic trait. However, because of the identical male palps (Figs 28–30 vs 31–33) and the small sampling size (single male), here we tentatively assign the Turkish specimen to *D. festai*, pending more thorough analyses.

Discussion

The red devil spiders are mostly restricted to the Western Palearctic, a region with a long taxonomic tradition and arguably with the best-catalogued biodiversity (Coddington & Levi 1991). In fact, the first description of a dysderid, *Harpactea hombergi* (Scopoli, 1763), was contemporary to Linnaeus. Additionally, red devil spiders are conspicuous, easy to distinguish from other spiders, relatively abundant, and easy to collect. Despite this, the taxonomy of Dysderidae remains contentious and descriptions usually lack an assessment of the intraspecific variability of diagnostic features, usually because they are either based on single specimens or single localities.

The combination of morphological evidence with a quantitative analysis of the phylogenetic relationships based on molecular data, provides unequivocal evidence that the genus *Dysderella* nests within *Dysdera*, and hence should be considered as its junior synonym. Additionally, the former species of *Dysderella* are shown to be closely related to species within the *longirostris* group, as already suggested by Deeleman-Reinhold & Deeleman? (1988). Interestingly, species of the *longirostris* group are mostly restricted to the Eastern Mediterranean and the Caucasus, with the single exception of *Dysdera ferghanica* Dunin, 1985 from Kyrgyzstan. The species formerly included in *Dysderella* expand the range of the bulk of the group towards the east, effectively bridging the biogeographic gap within the group.

Surprisingly, the phylogenetic analyses supported the placement of *D. kourosh* sp. nov. as a sister to species inhabiting the westernmost part of the distribution range of *Dysdera*. Judging from the morphology (e.g., distal segment of the bulb clearly longer than the proximal one, the well-developed crest, and the leg spination formula), the new species belongs to the *aculeata* group (sensu Deeleman-Reinhold & Deeleman 1988) which is mostly circumscribed to Central Asia. Unfortunately, the sparse species sampling precludes a quantitative biogeographic analysis of the genus. A more thorough sampling will be necessary to tackle this interesting biogeographic and evolutionary conundrum.

In conclusion, although undoubtedly increasing collecting efforts in poorly known and sparsely sampled regions will help to complete our understanding of the diversity of the red devil spiders, natural history collections across Europe hold large amounts of unsorted material from the western Palearctic. Brignoli's collection, now in the Museo Civico di Storia Naturale, Verona, keeps types of rare species from the Balkan Peninsula, Anatolia and Levantine region, many of which known only from the holotype (e.g., *D. sancticedri* comb. nov.). The collection of the Naturhistorisches Museum, Vienna, contains a lot of material from Turkey (incl. the Pontic Mountains), collected last century and still unidentified. In the present work, we have been able to prove that the species previously included in the genus *Dysderella* are nested inside *Dysdera*, the former being a junior synonymy, and describe three new species. Our study provides further evidence that the required information to tackle specific constraints in the family's classification might already exist within museum collections.

Acknowledgments

Dragomir Dimitrov thanks Peter Jäger (SMF, Frankfurt, Germany), Leonardo Latella (MCSN, Verona, Italy), and Christoph Hörweg (NHMW, Vienna, Austria) for giving him the opportunity to study the museum collections of the SMF, MCSM, and NHMW, respectively. Miquel Arnedo thanks Yuri M. Marusik

for sending him the specimen of *D. caspica*. The study was supported by Marie Skłodowska-Curie Individual Fellowship H2020-MSCA-IF-2019 (895672) funded by the European Commission and the projects "Cybertaxonomic approach to phylogenetic studies of model invertebrate genera (Invertebrata, Arachnida, Insecta), clarifying the problems of origin, formation, and conservation of the invertebrate fauna of the Balkan Peninsula", National Science Fund, Ministry of Education, Youth and Science of the Republic of Bulgaria, Grant KP-06-H21/1-17.12.2018 (Dragomir Dimitrov). Adrià Bellvert was funded by an individual Ph.D. Grant BES-2017- 080538 from the Ministerio de Economía, Industria y Competitividad of the Spanish government. Additional funding was provided by grant PID2019-105794GB from Ministerio de Economía y Competitividad of Spain, and 2017SGR83 from Agencia de Gestió d'Ajudes Universitàries, Catalonia (Miquel Arnedo).

References

Alicata P. 1964. Le specie italiane di Harpactocrates e di Parachtes n. gen. (Araneae, Dysderidae).

Alvarez-Padilla F. & Hormiga G. 2007. A protocol for digesting internal soft tissues and mounting spiders for scanning electron microscopy. *Journal of Arachnology* 35: 538–542. https://doi.org/10.1636/Sh06-55.1

Arnedo M.A., Oromi P. & Ribera C. 1996. Radiation of the genus Dysdera (Araneae, Haplogynae, Dysderidae) in the Canary Islands: The western islands. *Zoologica Scripta* 25 (3): 241–274. https://doi.org/10.1111/j.1463-6409.1996.tb00165.x

Arnedo M.A. & Ribera C. 1997. Radiation in the genus *Dysdera* (Araneae, Dysderidae) in the Canary Islands: The island of Gran Canaria. *Zoologica Scripta* 26: 205–243. https://doi.org/10.1111/j.1463-6409.1997.tb00413.x

Arnedo M.A. & Ribera C. 1999. Radiation in the genus *Dysdera* (Araneae, Dysderidae) in the Canary Islands: The island of Tenerife. *Journal of Arachnology* 27: 604–662.

Arnedo M.A., Oromí P. & Ribera C. 2000. Systematics of the genus *Dysdera* (Araneae, Dysderidae) in the eastern Canary Islands. *Journal of Arachnology*: 261–292. https://doi.org/10.1636/0161-8202(2000)028[0261:SOTGDA]2.0.CO;2

Arnedo M.A., Oromí P. & Ribera C. 2001. Radiation of the spider genus *Dysdera* (Araneae, Dysderidae) in the Canary Islands: Cladistic assessment based on multiple data sets. *Cladistics* 17 (4): 313–353. https://doi.org/10.1006/clad.2001.0168

Arnedo M.A., Oromí P., Múrria C., Macías-Hernández N. & Ribera C. 2007. The dark side of an island radiation: systematics and evolution of troglobitic spiders of the genus *Dysdera* Latreille (Araneae : Dysderidae) in the Canary Islands. *Invertebrate Systematics* 21 (6): 623–660. https://doi.org/10.1071/is07015

Bennett D.J., Hettling H., Silvestro D., Zizka A., Bacon C.D., Faurby S., Vos R.A. & Antonelli A. 2018. phylotaR: An automated pipeline for retrieving orthologous DNA sequences from GenBank in R. *Life* 8 (2): 1–11. https://doi.org/10.3390/life8020020

Bidegaray-Batista L. & Arnedo M.A. 2011. Gone with the plate: The opening of the Western Mediterranean basin drove the diversification of ground-dweller spiders. *BMC Evolutionary Biology* 11 (1). https://doi.org/10.1186/1471-2148-11-317

Brignoli P.M. 1978. Araignées du Liban IV. Notes sur quelques Dysderidae (Araneae). *Bulletin de la Société d'Histoire Naturelle de Toulouse* 114: 172–175.

Caporiacco L. di 1929. Aracnidi. *In*: Ricerche faunitische nelle isole italiane dell'Egeo. *Archivio Zoologico Italiano* 13: 221–242.

Charitonov D.E. 1956. Obzor paukov semeistva Dysderidae fauny SSSR. *Uchenye Zapiski Molotovskogo Gosudarstvennogo Universiteta Imeni A.M. Gor'kogo* 10: 17–39.

Coddington A. & Levi W. 1991. Systematics and evolution of spiders (Araneae). *Annual Review of Ecology and Systematics* 22: 565–592. https://doi.org/10.1146/annurev.es.22.110191.003025

Crespo L.C., Silva I., Enguídanos A., Cardoso P. & Arnedo M.A. 2021. Integrative taxonomic revision of the woodlouse-hunter spider genus *Dysdera* (Araneae: Dysderidae) in the Madeira archipelago with notes on its conservation status. *Zoological Journal of the Linnean Society* 192 (2): 356–415. https://doi.org/10.1093/zoolinnean/zlaa089

Dallwitz M.J. 1980. A general system for coding taxonomic descriptions. *Taxon* 29 (1): 41–46. https://doi.org/10.2307/1219595

Dallwitz M.J., Paine T.A. & Zurcher E.J. 2020. User's guide to the DELTA System: a general system for processing taxonomic descriptions. Available from https://www.delta-intkey.com/www/uguide.pdf [accessed 24 Jan. 2024].

Deeleman-Reinhold C.L. & Deeleman P.R. 1988. Revision des Dysderinae (Araneae, Dysderidae), les espèces mediterranéennes occidentales exceptées. *Tijdschrift voor Entomologie* 131: 141–269.

Dimitrov D. 2018. A Contribution to the study of Turkish Dysderidae with description of a new *Dysdera* (Araneae, Dysderidae). *Arachnology* 17 (9): 457–462. https://doi.org/10.13156/arac.2018.17.9.457

Dimitrov D. 2021. Description of *Dysdera zonsteini* n. sp. (Arachnida: Araneae: Dysderidae) from Turkmenistan. *Zootaxa* 4938 (5): 588–594. https://doi.org/10.11646/zootaxa.4938.5.6

Doblika K. 1853. Beitrag zur Monographie des Spinnengeschlechtes *Dysdera*. *Verhandlungen des zoologisch-botanischen Vereins in Wien* 3: 115–124.

Dunin P.M. 1985. The spider family Dysderidae (Aranei, Haplogynae) in the Soviet Central Asia. *Trudy Zoologicheskogo Instituta Akademii Nauk SSSR, Leningrad* 139: 114–120.

Dunin P.M. 1990. Spiders of the genus *Dysdera* (Aranei, Haplogynae, Dysderidae) from Azerbaijan. *Zoologicheskiĭ Zhurnal* 69 (6): 141–148.

Dunin P.M. 1992. The spider family Dysderidae of the Caucasian fauna (Arachnida Aranei Haplogynae). *Arthropoda Selecta* 1 (3): 35–76.

Dunin P.M. & Fet V.Y. 1985. *Dysdera transcaspica* sp. n. (Aranei, Dysderidae) from Turkmenia. *Zoologicheskiĭ Zhurnal* 64: 298–300.

Ernst M., Jønsson K.A., Ericson P.G.P., Blom M.P.K. & Irestedt M. 2022. Utilizing museomics to trace the complex history and species boundaries in an avian-study system of conservation concern. *Heredity* 128 (3): 159–168. https://doi.org/10.1038/s41437-022-00499-0

Fomichev A.A. & Marusik Y.M. 2021. Notes on the spider genus *Dysdera* Latreille, 1804 (Araneae: Dysderidae) in Central Asia. *Zootaxa* 5006 (1): 73–89. https://doi.org/10.11646/zootaxa.5006.1.10

Goloboff P.A. & Catalano S.A. 2016. TNT version 1.5, including a full implementation of phylogenetic morphometrics. *Cladistics* 32 (3): 221–238. https://doi.org/10.1111/cla.12160

Hoang D.T., Chernomor O., Von Haeseler A., Minh B.Q. & Vinh L.S. 2018. UFBoot2: Improving the ultrafast bootstrap approximation. *Molecular Biology and Evolution* 35 (2): 518–522. https://doi.org/10.1093/molbev/msx281

Holmgren S., Angus R., Jia F., Chen Z.N. & Bergsten J. 2016. Resolving the taxonomic conundrum in *Graphoderus* of the east Palearctic with a key to all species (Coleoptera, Dytiscidae). *ZooKeys* 2016 (574): 113–142. https://doi.org/10.3897/zookeys.574.7002

Kalyaanamoorthy S., Minh B.Q., Wong T.K.F., Von Haeseler A. & Jermiin L.S. 2017. ModelFinder: Fast model selection for accurate phylogenetic estimates. *Nature Methods* 14 (6): 587–589. https://doi.org/10.1038/nmeth.4285

Katoh K. & Standley D.M. 2013. MAFFT multiple sequence alignment software version 7: Improvements in performance and usability. *Molecular Biology and Evolution* 30 (4): 772–780. https://doi.org/10.1093/molbev/mst010

Kroneberg A. 1875. Araneae. *In*: Fedtschenko A.P. (ed.) Puteshestvie v Tourkestan. Reisen in Turkestan. Zoologischer Theil. *Nachrichten der Gesellschaft der Freunde der Naturwissenschaften zu Moskau* 19 (3): 1–58.

Lanfear R., Frandsen P.B., Wright A.M., Senfeld T. & Calcott B. 2017. Partitionfinder 2: New methods for selecting partitioned models of evolution for molecular and morphological phylogenetic analyses. *Molecular Biology and Evolution* 34 (3): 772–773. https://doi.org/10.1093/molbev/msw260

Latreille P.A. 1804. Tableau méthodique des insectes. *Nouveau Dictionnaire d'Histoire Naturelle Paris* 24: 129–295.

Lazarov S. 2009. A new record of *Dysdera tartarica* Kroneberg, 1875 with a description of the previously unknown female (Araneae, Dysderidae). *Turkish Journal of Arachnology* 1 (2, for 2008): 104–106.

Macías-Hernández N., Oromí P. & Arnedo M.A. 2010. Integrative taxonomy uncovers hidden species diversity in woodlouse hunter spiders (Araneae, Dysderidae) endemic to the Macaronesian archipelagos. *Systematics and Biodiversity* 8 (4): 531–553. https://doi.org/10.1080/14772000.2010.535865

Michalik P., Kallal R.J., Dederichs T.M., Labarque F.M., Hormiga G., Giribet G. & Ramírez M.J. 2019. Phylogenomics and genital morphology of cave raptor spiders (Araneae, Trogloraptoridae) reveal an independent origin of a flow-through female genital system. *Journal of Zoological Systematics and Evolutionary Research* 57 (4): 737–747. https://doi.org/10.1111/jzs.12315

Minh B.Q., Schmidt H.A., Chernomor O., Schrempf D., Woodhams M.D., Von Haeseler A., Lanfear R. & Teeling E. 2020. IQ-TREE 2: New models and efficient methods for phylogenetic inference in the genomic era. *Molecular Biology and Evolution* 37 (5): 1530–1534. https://doi.org/10.1093/molbev/msaa015

Müller K. 2005. SeqState. *Applied Bioinformatics* 4 (1): 65–69. https://doi.org/10.2165/00822942-200504010-00008

Nosek A. 1905. Araneiden, Opilionen und Chernetiden. *In*: Penther A. & Zederbauer E. (eds) *Ergebnisse einer naturwissenschaftlichen Reise zum Erdschias-Dagh (Kleinasien). Annalen des Kaiserlich-Königlichen Naturhistorischen Hofmuseums in Wien*: 20: 114–154.

Rambaut A., Drummond A.J., Xie D., Baele G. & Suchard M.A. 2018. Posterior summarization in Bayesian phylogenetics using Tracer 1.7. *Systematic Biology* 67 (5): 901–904. https://doi.org/10.1093/sysbio/syy032

Raxworthy C.J. & Smith B.T. 2021. Mining museums for historical DNA: advances and challenges in museomics. *Trends in Ecology and Evolution* 36 (11): 1049–1060. https://doi.org/10.1016/j.tree.2021.07.009

Řezáč M., Cardoso P. & Řezáčová V. 2023. Review of *Harpactea* ground-dwelling spiders (Araneae: Dysderidae) of Portugal. *Zootaxa* 5263 (3): 335–364. https://doi.org/10.11646/zootaxa.5263.3.2

Ronquist F., Teslenko M., Van Der Mark P., Ayres D.L., Darling A., Höhna S., Larget B., Liu L., Suchard M.A. & Huelsenbeck J.P. 2012. Mrbayes 3.2: Efficient bayesian phylogenetic inference and model choice across a large model space. *Systematic Biology* 61 (3): 539–542. https://doi.org/10.1093/sysbio/sys029

Scharff N. & Hormiga G. 2013. On the Australian linyphiid spider *Alaxchelicera ordinaria* Butler, 1932 (Araneae). *Zootaxa* 3750 (2): 193–196. https://doi.org/10.11646/zootaxa.3750.2.8

Scopoli J.A. 1763. *Entomologia Carniolica, exhibens insecta Carniolae indigena et distributa in ordines, genera, species, varietates: methodo Linnaeana.* Ioannis Thomae Trattner, Vindobonae [= Johannes Thomas Trattner, Wien/Vienna]. https://doi.org/10.5962/bhl.title.34434

Simmons M.P. & Ochoterena H. 2000. Gaps as characters in sequence-based phylogenetic analyses. *Systematic Biology* 49 (2): 369–381. https://doi.org/10.1093/sysbio/49.2.369

Simon E. 1882. Etudes arachnologiques. 13e Mémoire. XX. Descriptions d'espèces et de genres nouveaux de la famille des Dysderidae. *Annales de la Société Entomologique de France (6)* 2: 201–240.

Simon E. 1911. Catalogue raisonné des arachnides du nord de l'Afrique (1re partie). *Annales de la Société Entomologique de France* 79 (3, 1910): 265–332.

Soto E.M., Labarque F.M., Ceccarelli F.S., Arnedo M.A., Pizarro-Araya J. & Ramírez M.J. 2017. The life and adventures of an eight-legged castaway: Colonization and diversification of *Philisca* ghost spiders on Robinson Crusoe Island (Araneae, Anyphaenidae). *Molecular Phylogenetics and Evolution* 107: 132–141. https://doi.org/10.1016/j.ympev.2016.10.017

Thorell T. 1875. Diagnoses Aranearum Europaearum aliquot novarum. *Tijdschrift voor Entomologie* 18: 81–108.

Twort V.G., Minet J., Wheat C.W. & Wahlberg N. 2021. Museomics of a rare taxon: placing Whalleyanidae in the Lepidoptera Tree of Life. *Systematic Entomology* 46 (4): 926–937. https://doi.org/10.1111/syen.12503

Vaidya G., Lohman D.J. & Meier R. 2011. SequenceMatrix: concatenation software for the fast assembly of multi-gene datasets with character set and codon information. *Cladistics* 27 (2): 171–180. https://doi.org/10.1111/j.1096-0031.2010.00329.x

World Spider Catalog 2023. World Spider Catalog. Version 24. Natural History Museum Bern. https://doi.org/10.24436/2

Zamani A., Marusik Y.M. & Szűts T. 2023a. A survey of *Dysderella* Dunin, 1992 (Araneae, Dysderidae), with a new species from Iran. *Zoosystematics and Evolution* 99 (2): 337–344. https://doi.org/10.3897/zse.99.104613

Zamani A., Marusik Y.M. & Szűts T. 2023b. A survey of the spider genus *Dysdera* Latreille, 1804 (Araneae, Dysderidae) in Iran, with fourteen new species and notes on two fossil genera. 86: 43–86. https://doi.org/10.3897/zookeys.1146.97517

Manuscript received: 16 May 2023
Manuscript accepted: 14 September 2023
Published on: 14 February 2024
Topical editor: Magalie Castelin
Section editor: Rudy Jocqué
Desk editor: Radka Rosenbaumová

Supplementary files

Supp. file 1. Specimen and sequence information.
https://doi.org/10.5852/ejt.2024.921.2429.10753

Supp. file 2. Supplementary figures. **SFig. 1**. Maximum likelihood tree inferred with bet partion scheme and models in IQTREE2. Numbers on nodes refer to ultrafast bootstrap values. **SFig. 2**. Majority rule consensus tree inferred with MrBayes with the best partion scheme and models as selected by PartionFinder. **SFig. 3**. Strict consensus tree of most parsimonious trees as inferred with TNT. Numbers on nodes refer to jack-knife values.
https://doi.org/10.5852/ejt.2024.921.2429.10755

Supp. file 3. List of partition schemes and corresponding preferred evolutionary models used in the analyses.
https://doi.org/10.5852/ejt.2024.921.2429.10757